

The First Five Minutes of a Core Collapse Supernova: Multidimensional Hydrodynamic Models

K. Kifonidis¹, T. Plewa^{2,1}, H.-Th. Janka¹, E. Müller¹

¹ *Max-Planck-Institut für Astrophysik, Karl-Schwarzschild-Strasse 1, D-85740 Garching, Germany*

² *Nicolaus Copernicus Astronomical Center, Bartycka 18, 00716 Warsaw, Poland*

1 Introduction

Numerous observations of SN 1987 A suggest that extensive mixing has taken place in the exploding envelope of the progenitor star Sk -69 202. The early detection of X and γ -rays, the broad profiles of infrared Fe and Co lines, as well as the shape of the light curve cannot be explained without assuming that clumps of newly synthesized ^{56}Ni , from layers close to the collapsed core, have penetrated into the hydrogen envelope (see the reviews of Arnett et al. 1989 and Müller 1998, and the references therein). That such mixing is probably generic in core collapse supernovae is indicated by spectroscopic studies of SN 1987 F, SN 1988 A, SN 1993 J (Spyromilio, 1994, and references therein) and SN 1995 V (Fassia et al., 1998). Furthermore, it might also explain the detection of fast moving clumps of metal-enriched material in the Vela (Aschenbach et al., 1995), Cas A (Anderson et al., 1994) and Puppis A (Winkler & Kirshner, 1985) supernova remnants as well as the isotopic composition of specific SiC grains with possible supernova origin found in primitive meteorites (Nittler et al. 1996; Amari this volume). But even more important from the point of view of supernova modellers is the fact, that a detailed understanding of the problem of nucleosynthesis and mixing can give us invaluable information about the explosion mechanism itself. Thus, the observations have instigated theoretical work on multidimensional supernova models which focused either on the role of convection occurring within the first second of a delayed, neutrino-driven explosion (Mezzacappa et al., 1998; Janka & Müller, 1996; Burrows et al., 1995; Herant et al., 1994; Miller et al., 1993), or on the growth of Rayleigh-Taylor instabilities during the late evolutionary stages (Nagataki et al., 1998; Herant & Benz, 1992; Müller et al., 1991; Yamada & Sato, 1991; Hachisu et al., 1990).

However, multidimensional simulations which follow the evolution of the stalled supernova shock from its revival due to neutrino heating, until its emergence from the stellar surface have not yet been performed. Due to the presence of vastly different spatial and temporal scales and the range of physical processes involved during the early stages following core collapse, all studies of mixing in core collapse supernovae have hitherto neglected the influence of neutrino-driven convection in seeding the Rayleigh-Taylor instabilities. Instead, a shock wave was created artificially by depositing the explosion energy near the center of a pre-collapse progenitor model and following the propagation of the shock in one spatial dimension until it had reached one of the unstable composition interfaces. This was either chosen to be the He/H interface in case of Type II supernova models (e.g. Herant & Benz 1992; Müller et al. 1991) or the C+O/He interface in case of Type Ib models (Hachisu et al., 1994). Only then were the 1D models mapped to a 2D grid and the rest of the evolution followed with a multidimensional code. A somewhat different, two-dimensional approach, was chosen in the recent calculations of Nagataki et al. (1997) who initiated the explosion using a parameterized, aspherical shock wave and computed the resulting nucleosynthesis using a marker particle approximation. These models have been subsequently used by Nagataki et al. (1998) for a study of Rayleigh-Taylor instabilities at the He/H interface. Still, however, these calculations do not address the complications introduced by the explosion mechanism and thus suffer from a number of assumptions. Furthermore, their numerical resolution appears to be hardly sufficient to resolve instabilities which occur within the first minutes of the evolution.

In the present contribution a first step towards a more consistent multidimensional picture of core collapse supernovae is attempted by trying to answer the questions

- What happens in the first minutes and hours of a core collapse supernova *if* neutrino heating indeed succeeds in reviving the supernova shock?
- Can neutrino-driven convection in conjunction with the later Rayleigh-Taylor instabilities lead to the high iron velocities observed in SN 1987A?

For this purpose we have carried out high-resolution 2D supernova simulations which for the first time cover the neutrino-driven initiation of the explosion, the accompanying convection and nucleosynthesis as well as the Rayleigh-Taylor mixing. In the following, we present preliminary results from these calculations, focusing on the first ~ 300 seconds of evolution. A summary of our work can also be found in Kifonidis et al. (1999).

2 Numerical Method and Initial Data

We split our simulation into two stages. The early evolution ($t \leq 1$ s) which encompasses shock revival by neutrino heating, neutrino-driven convection and explosive nucleosynthesis is followed with a version of the HERAKLES code (T. Plewa & E. Müller, in preparation). This hydrodynamics code solves the multidimensional hydrodynamic equations using the direct Eulerian version of the Piecewise Parabolic Method (Colella & Woodward, 1984) augmented by the Consistent Multifluid Advection (CMA) scheme of Plewa & Müller (1999) in order to guarantee exact conservation of nuclear species. We have added the input physics (neutrino source terms, equation of state, boundary conditions, gravitational solver) described in Janka & Müller (1996) (henceforth JM96) with the following modifications. General relativistic corrections are made to the gravitational potential following Van Riper (1979). A 14-isotope network is incorporated in order to compute the explosive nucleosynthesis. It includes the 13 α -nuclei from ^4He to ^{56}Ni and a representative tracer nucleus which is used to monitor the distribution of the neutrino-heated, neutron-rich material and to replace the ^{56}Ni production when Y_e drops below ~ 0.49 (cf. Thielemann et al., 1996).

We start our calculations 20 ms after core bounce from a model of Bruenn (1993) who has followed core-collapse and bounce in the $15 M_\odot$ progenitor model of Woosley et al. (1988). The model is mapped to a 2D grid consisting of 400 radial zones ($3.17 \times 10^6 \text{ cm} \leq r \leq 1.7 \times 10^9 \text{ cm}$), and 180 angular zones ($0 \leq \theta \leq \pi$; cf. JM96 for details). A random initial seed perturbation is added to the velocity field with a modulus of 10^{-3} of the (radial) velocity of Bruenn’s post-collapse model. The calculations are carried up to 885 ms. At this time the explosion energy has saturated and essentially all nuclear reactions have frozen out. We will henceforth refer to this calculation as our “explosion model”.

The subsequent shock propagation through the stellar envelope and the growth of Rayleigh-Taylor instabilities is followed with the AMRA Adaptive Mesh Refinement (AMR) code (T. Plewa & E. Müller, in preparation). This code uses a different variant of HERAKLES as its hydrodynamics solver which does not include the neutrino physics. Gravity is neglected in the AMR calculations since, as is the case for the neutrino source terms, it does not influence the propagation of the shock during late evolutionary stages. However, gravity is important for determining the amount of fallback, a problem which is outside the scope of the present study. The equation of state takes into account contributions from photons, non-degenerate electrons, e^+e^- -pairs, ^1H , and the nuclei included in the reaction network. The AMR calculations are started with the inner and outer boundaries located at $r_{\text{in}} = 10^8 \text{ cm}$ (i.e. inside the hot bubble containing the neutrino-driven wind) and $r_{\text{out}} = 2 \times 10^{10} \text{ cm}$, respectively. No further seed perturbations are added. We use up to four levels of mesh refinement and refinement factors of four in each grid direction, yielding a maximum resolution equivalent to that of a uniform grid of 3072×768 zones. In order to keep the radial resolution as high as possible during any given evolutionary time, we do not include the entire star but allow the code to expand the radial extent of the base grid by a factor of 2 to 4 whenever the supernova shock is approaching the outer grid boundary. The latter is moved from

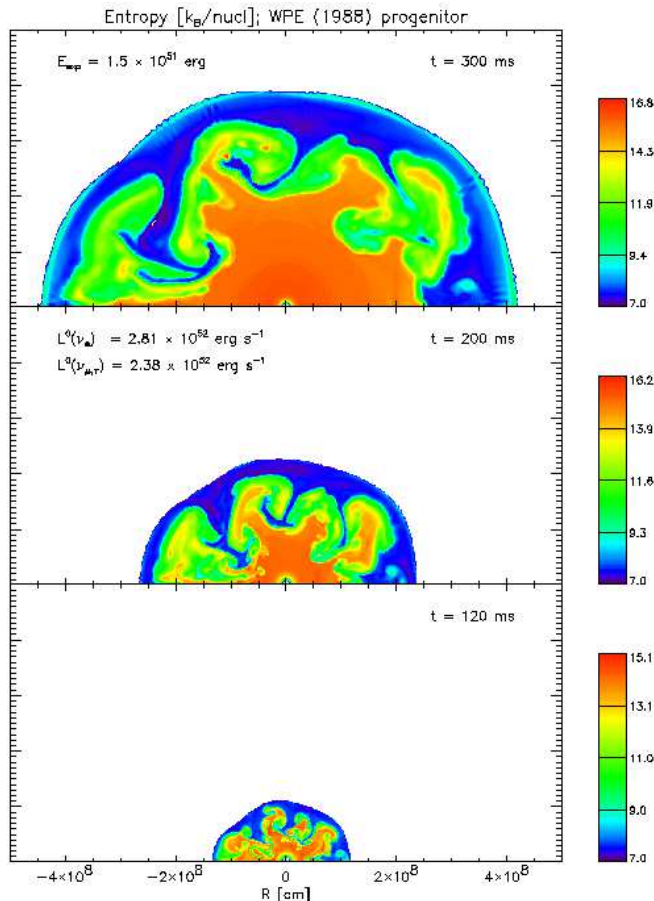


Figure 1: Evolution of the entropy in our explosion model within the first 300ms after the start of the calculations. Neutrino-heated, deleptonized material rises in large bubbles and distorts the shock (outermost discontinuity).

its initial value out to $r_{\text{out}} = 1.1 \times 10^{12}$ cm at $t = 300$ s. Reflecting boundary conditions are used at $\theta = 0$ and $\theta = \pi$ and free outflow is allowed across the inner and outer radial boundaries.

3 Nucleosynthesis and Neutrino-Driven Convection

The general features of our explosion model are comparable to the models of JM96. For the initial neutrino luminosities, which are prescribed at the inner boundary, somewhat below the neutrino sphere, and decay with time as described in JM96, we have adopted a value of $L_{\nu_e}^0 = 2.8125 \times 10^{52}$ erg/s for the electron neutrinos and $L_{\nu_x}^0 = 2.375 \times 10^{52}$ erg/s for the heavy lepton neutrinos (with $\nu_x = \nu_\mu, \bar{\nu}_\mu, \nu_\tau, \bar{\nu}_\tau$). The parameters describing lepton and energy loss of the inner iron core were set to $\Delta Y_l^i = 0.0875$, $\Delta \varepsilon = 0.0625$ (cf. JM96). The neutrino spectra are the same as in JM96.

For the chosen neutrino luminosities the shock starts to move out of the iron core almost immediately. Convection between shock and gain radius sets in ~ 30 ms after the start of the simulation in form of rising blobs of neutrino-heated, deleptonized material (with $Y_e \ll 0.5$) separated by narrow downflows with $Y_e \approx 0.49$ (Fig. 1). The shock reaches the Fe/Si interface at $r = 1.4 \times 10^8$ cm after ~ 100 ms. Shortly thereafter, at $t \approx 120$ ms temperatures right behind the shock have dropped below $\approx 7 \times 10^9$ K, and ^{56}Ni starts to form in a narrow shell (Fig. 2).

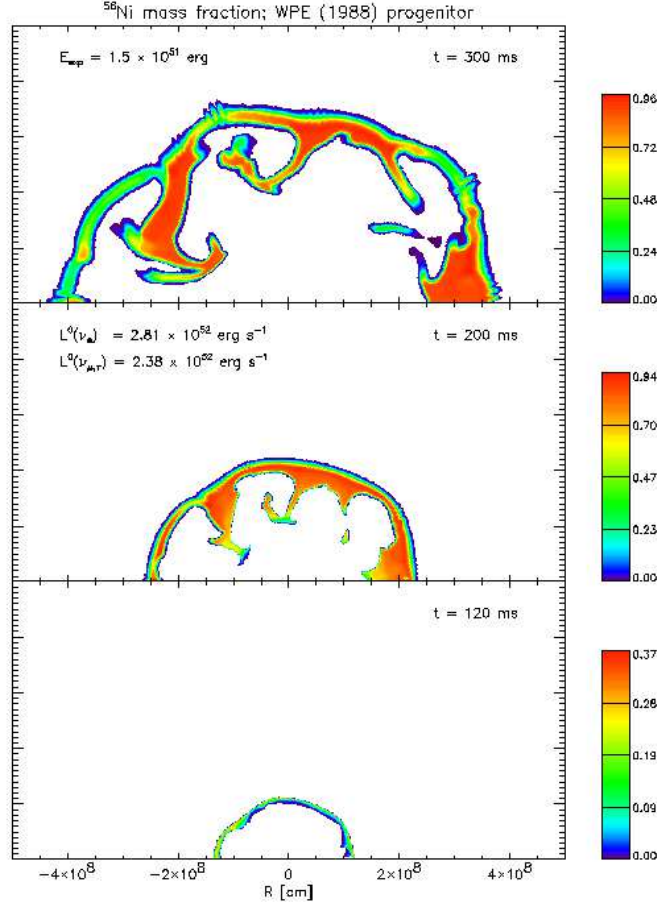


Figure 2: Evolution of the ^{56}Ni mass fraction within the first 300 ms after the start of the calculations. ^{56}Ni has only been synthesized in those regions which have an electron fraction $Y_e > 0.49$ and reached peak-temperatures above $\sim 5 \times 10^9$ K.

During the ongoing expansion and cooling, ^{56}Ni is also synthesized in the convective region. However, its synthesis proceeds exclusively in the narrow downflows which separate the rising bubbles and have a sufficiently high electron fraction Y_e . This leads to a highly inhomogeneous nickel distribution (middle panel of Fig. 2) shortly before complete silicon burning freezes out at $t \approx 250$ ms. Moreover, convective motions are still present even after ^{56}Ni production ceases, and distort the nickel containing shell (upper panel of Fig. 2). Only when convection stops around $t \approx 400$ ms, the flow pattern becomes frozen in and the entire post-shock region expands nearly uniformly.

Due to the asphericity of the shock caused by the rising bubbles, “bent” shells containing the products of incomplete silicon burning as well as oxygen burning form outside the nickel-enriched region. The post-shock temperature drops below 2.8×10^9 K at $t = 495$ ms, when the shock is about to cross the Si/O interface. Thus, our model shows only moderate oxygen burning (due to a non-vanishing oxygen abundance in the silicon shell), and negligible neon and carbon burning. This is caused by the specific structure of the progenitor model of Woosley et al. (1988) and may change when different (especially more massive) progenitors are used. In total, $0.052 M_\odot$ of ^{56}Ni are produced, while $0.10 M_\odot$ of material in the deleptonized bubbles are synthesized at conditions with $Y_e < 0.49$ and end up as neutron-rich nuclei. The explosion energy of our 2D model saturates at 1.48×10^{51} erg at $t = 885$ ms. This value is still to be corrected for the binding energy of the

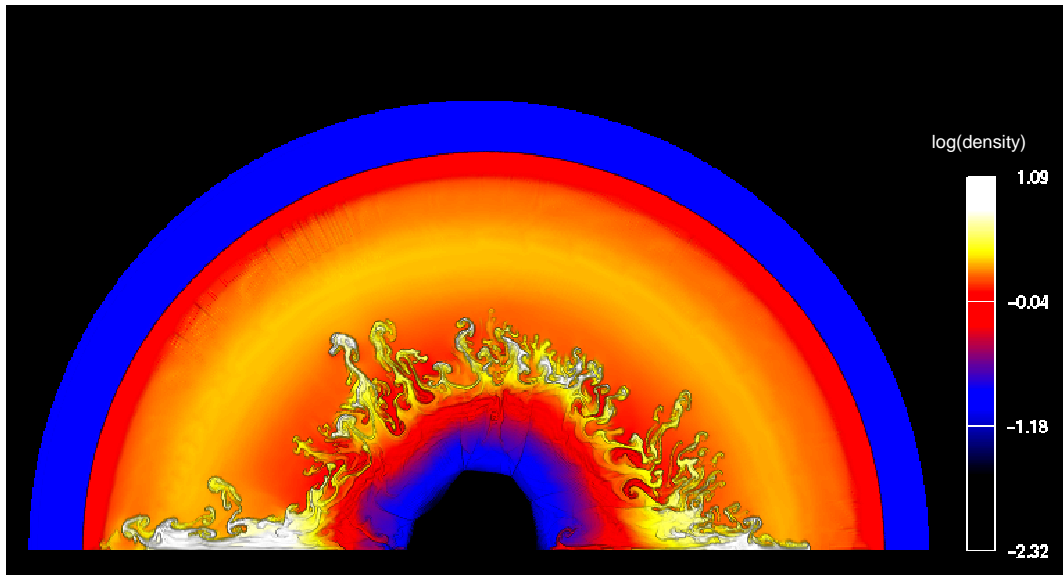


Figure 3: Density distribution ($\log_{10} \rho$ [g cm^{-3}]) in the exploding star, 100 s after core bounce. The outer edge of the displayed domain (blue) coincides with a radius of 1.15×10^{11} cm. The supernova shock (bright orange discontinuity near the outer edge) has crossed the He/H-interface and reached a radius of $r = 10^{11}$ cm. Rayleigh-Taylor mushrooms distribute the products of explosive nucleosynthesis throughout the He-core. The reverse shock (aspherical discontinuity) visible near the center was created after the main shock had passed the C+O/He-interface of the star. (The excessive outflows along the axis are specific to the use of polar coordinates.)

outer envelope.

4 Growth of Rayleigh-Taylor Instabilities

During the next seconds the shock detaches from the formerly convective shell that carries the products of explosive nucleosynthesis, loses its asphericity and crosses the C+O/He-interface. Along with the slow-down which the shock experiences after passing this interface due to the varying density gradient, the entire post-shock material is also rapidly decelerated. Twenty seconds after core-bounce, the metal-containing shell has thus been compressed to a thin, dense layer which is bounded inwards by a reverse shock and contains two regions which show crossed density and pressure gradients. The first of these is located at the Ni+Si/O-interface while the second coincides with the C+O/He-interface. Thus, Rayleigh-Taylor instabilities at the Ni+Si/O and C+O/He-interfaces grow rapidly.

At $t = 100$ s (Fig. 3) the instabilities are fully developed and have already interacted with each other. Nickel and silicon are dragged upward into the helium shell in rising mushrooms on angular scales from 1° to about 5° , whereas helium is mixed inward in bubbles. Oxygen and carbon, located in intermediate layers of the progenitor, are swept outward as well as inward in rising and sinking flows. At $t = 300$ s the densities between the dense mushrooms and the ambient medium differ by factors up to 5 while the fastest mushrooms have already propagated out to more than half the radius of the He core (Fig. 4).

We observe that the nickel is born with very high velocities, of the order of 15,000 km/s at $t = 300$ ms. These velocities drop significantly during the subsequent evolution, especially after the shock passes the C+O/He interface. At a time of $t = 50$ s most of the ^{56}Ni is expanding with 3200 – 4500 km/s and maximum velocities $v_{\text{Ni}}^{\text{max}}$ are around 5800 km/s. During the following 50

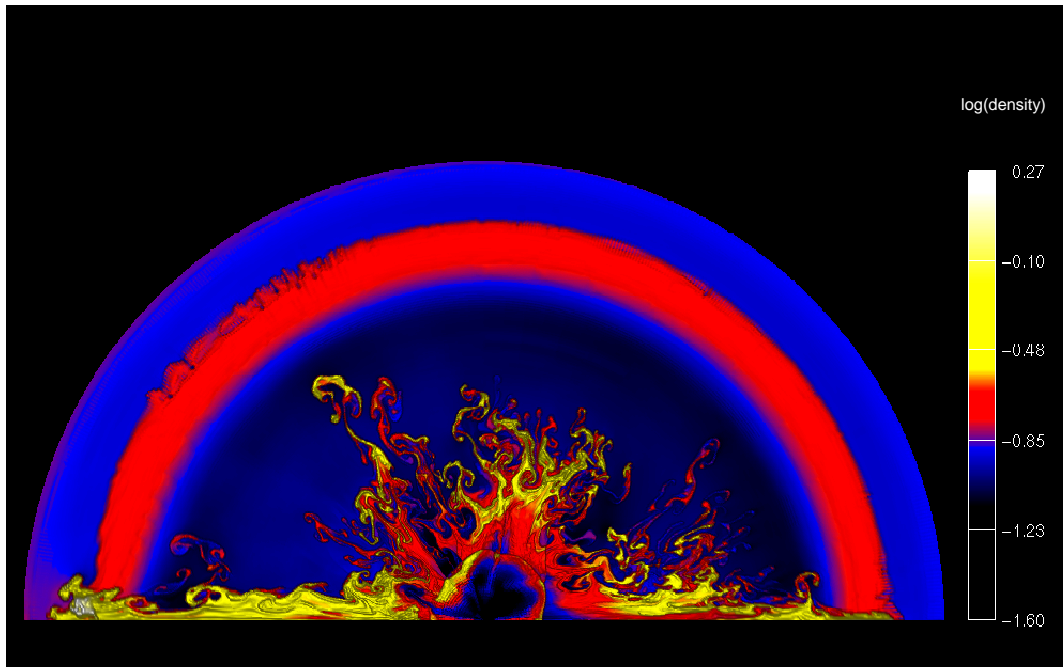


Figure 4: Density distribution ($\log_{10} \rho$ [g cm^{-3}]) 300 s after core bounce in the inner $\sim 3 \times 10^{11}$ cm of the star. The supernova shock (outermost blue discontinuity) is located inside the hydrogen envelope at $r = 2.7 \times 10^{11}$ cm. A dense shell (visible as a bright red ring) has formed behind the shock. Its outer boundary coincides with the He/H interface while its inner boundary is in the process of steepening into a reverse shock. The fastest mushrooms have almost caught up with the inner boundary of the shell. (The excessive outflows along the axis are specific to the use of polar coordinates.)

seconds, $v_{\text{Ni}}^{\text{max}}$ drops to ~ 5000 km/s. However, after $t = 100$ s, the clumps start to move essentially ballistically through the helium core and only a slight decrease of $v_{\text{Ni}}^{\text{max}}$ to ~ 4700 km/s occurs until 300 s, when the bulk of ^{56}Ni has velocities below 3000 km/s.

We have recently accomplished to follow the subsequent evolution of our model up to 16 000 s after core-bounce. The unsteady propagation speed of the supernova shock which has formerly induced the instability at the Ni+Si/O and C+O/He-interfaces also leads to the formation of a dense (Rayleigh-Taylor unstable) shell at the He/H interface. As before, the inner boundary of this shell steepens into a reverse shock (Fig. 4), while in the process of this the entire shell is rapidly slowed down. Our high-resolution simulations reveal a potentially severe problem for the mixing of heavy elements into the hydrogen envelope of Type II supernovae like SN 1987A. We find that the fast nickel containing clumps, after having penetrated through this reverse shock, dissipate a large fraction of their kinetic energy in bow shocks created by their supersonic motion through the shell medium. This leads to their deceleration to ~ 2000 km/s in our calculations. Contrary to all previous studies, which tried to *accelerate* the nickel by the instabilities, our computations show, that the main problem for obtaining high nickel velocities is how to avoid *decelerating* the clumps once they reach the He/H interface. The growth time scale of the instability at this interface is too large to allow for a fast shredding of the dense shell and the formation of “holes” through which the clumps could penetrate more easily. The high iron velocities in SN 1987 A might therefore hint towards a smoother density profile exterior to the He-core, which would suppress dense shell formation, or towards a global asymmetry of the explosion.

During the computations we became aware of oscillations with angle in parts of the postshock flow (Figs. 2 and 4). These are caused by the “odd-even decoupling” phenomenon associated with

grid-aligned shocks (Quirk 1994; see also LeVeque 1998). As a consequence, the maximum nickel velocities, $v_{\text{Ni}}^{\text{max}}$, obtained in our AMR calculations have probably been overestimated by $\sim 25\%$ because the growth of some of the mushrooms was influenced by the perturbations induced by this numerical defect. The main results of our study, however, are not affected.

5 Conclusions

We have studied the evolution of a core collapse supernova in a $15 M_{\odot}$ blue supergiant progenitor focusing on the first 300s after core bounce. As a result of the interplay between neutrino-matter interactions, hydrodynamic instabilities and nucleosynthesis in the framework of the neutrino-driven explosion mechanism, the products of explosive silicon and oxygen burning are mixed throughout the inner half of the helium core of the progenitor star. Ballistically moving, metal-enriched clumps with velocities up to more than ~ 4000 km/s are observed. Rayleigh-Taylor instabilities at the C+O/He and Ni+Si/O-interfaces transport helium deep inward and sweep nickel, silicon, oxygen and carbon outward in rising mushrooms.

Our simulations suggest that high-velocity metal-rich clumps are ejected during the explosion of Type Ib (and Ic) supernovae. In case of Type II supernovae, however, the dense shell left behind by the shock passing the boundary between helium core and hydrogen envelope, causes a substantial deceleration of the clumps. Thus, we cannot confirm the results of Herant & Benz (1992) that “premixing” of the ^{56}Ni within the first minutes of the explosion, and its later interaction with the instability at the He/H-interface, can explain the high iron velocities observed in SN 1987A. Moreover, our calculations strongly indicate, that all computations of Rayleigh-Taylor mixing in Type II supernovae carried out so far (including the case of SN 1987A) have been started from *overly simplified* initial conditions since they have neglected clump formation during the first minutes of the explosion. In future work, it will be most interesting to study how the discussed effects depend on different progenitor models and to explore the implications of the strong outward mixing of ^{56}Ni for the light curves and spectra of Type Ib supernovae.

Acknowledgements

We are very grateful to Stanford Woosley for providing us with the progenitor model used in this study as well as for stimulating discussions about Type Ib supernovae. We thank S. Bruenn for making available the data of his post-bounce model and P. Ciecieląg and R. Walder for their help regarding visualization. The work of TP was partly supported by grant KBN 2.P03D.004.13 from the Polish Committee for Scientific Research. The simulations were performed on the NEC SX-4B and CRAY J916/16512 of the Rechenzentrum Garching.

References

- Arnett, W. D., Bahcall, J. N., Kirshner, R. P., Woosley, S. E. 1989, *Ann. Rev. Astron. Astrophys.*, 27, 341
- Anderson, M. C., Jones, T. W., Rudnick, L., Tregilis, I. L., and Kang, H. 1994, *ApJ*, 421, L31
- Aschenbach, B., Egger, R., and Trümper, J. 1995, *Nature*, 373, 587
- Bruenn, S. W. 1993, *Nuclear Physics in the Universe*, M. W. Guidry and M. R. Strayer, Bristol: IOP, 1993, 31
- Burrows, A., Hayes, J., and Fryxell, B. A. 1995, *ApJ*, 450, 830
- Colella, P., and Woodward, P. R. 1984, *J. Comput. Phys.*, 54, 174

- Fassia, A., Meikle, W. P. S., Geballe, T. R., Walton, N. A., Pollacco, D. L., Rutten, R. G. M., and Tinney, C. 1998, MNRAS, 299, 150
- Hachisu, I., Matsuda, T., Nomoto, K., and Shigeyama, T. 1990, ApJ, 358, L57
- Hachisu, I., Matsuda, T., Nomoto, K., and Shigeyama, T. 1994, A&AS, 104, 341
- Herant, M., and Benz, W. 1992, ApJ, 387, 294
- Herant, M., Benz, W., Hix, W. R., Fryer, C. L., and Colgate, S. A. 1994, ApJ, 435, 339
- Janka, H.-Th., and Müller, E. 1996, A&A, 306, 167 (JM96)
- Kifonidis, K., Plewa, T., Janka, H.-Th., and Müller, E. 1999, ApJ, submitted (astro-ph/9911183)
- LeVeque, R. J. 1998, Computational Methods for Astrophysical Fluid Flow, O. Steiner and A. Gautschy, Berlin: Springer, 1998, 116
- Mezzacappa, A., Calder, A. C., Bruenn, S. W., Blondin, J. M., Guidry, M. W., Strayer, M. R., and Umar, A. S. 1998, ApJ, 495, 911
- Miller, D. S., Wilson, J. R., and Mayle, R. W. 1993, ApJ, 415, 278
- Müller, E. 1998, Computational Methods for Astrophysical Fluid Flow, O. Steiner and A. Gautschy, Berlin: Springer, 1998, 371
- Müller, E., Fryxell, B. A., and Arnett, W. D. 1991, A&A, 251, 505
- Nagataki, S., Hashimoto, M., Sato, K., and Yamada, S. 1997, ApJ, 486, 1026
- Nagataki, S., Shimizu, T. M., and Sato, K. 1998, ApJ, 495, 413
- Nittler, L. R., Amari, S., Zinner, E., Woosley, S. E., and Lewis, R. S. 1996, ApJ, 462, L31
- Plewa, T., and Müller, E. 1999, A&A, 342, 179
- Quirk, J. J. 1994, Int. J. Num. Meth. Fluids, 18, 555
- Spyromilio, J. 1994, MNRAS, 266, L61
- Thielemann, F.-K., Nomoto, K., and Hashimoto, M. 1996, ApJ, 460, 408
- Van Riper, K. A. 1979, ApJ, 232, 558
- Winkler, P. F., and Kirshner, R. P. 1985, ApJ, 299, 981
- Woosley, S. E., Pinto, P. A., and Ensman, L. 1988, ApJ, 324, 466
- Yamada, S., and Sato, K. 1991, ApJ, 382, 594